

Supplementary Materials for:

Dynamic Shear Rheology of a Thixotropic Suspension: Comparison of an Improved Structure-Based Model with Large Amplitude Oscillatory Shear Experiments

Matthew J. Armstrong, Antony N. Beris, Simon A. Rogers, Norman J. Wagner^{a)}

Journal of Rheology, 2016

1) Yield Stress and Elastic Stress Determination

Fig. S.1a shows a series of static yield stress experiments to validate the yield stress [Dullaert and Mewis (2005d)]. The elastic stress was determined during steady shear flow following the procedures from Dullaert and Mewis (2005d). Fig. S.1b shows the determination of the elastic stress contributions for the six shear rates shown.

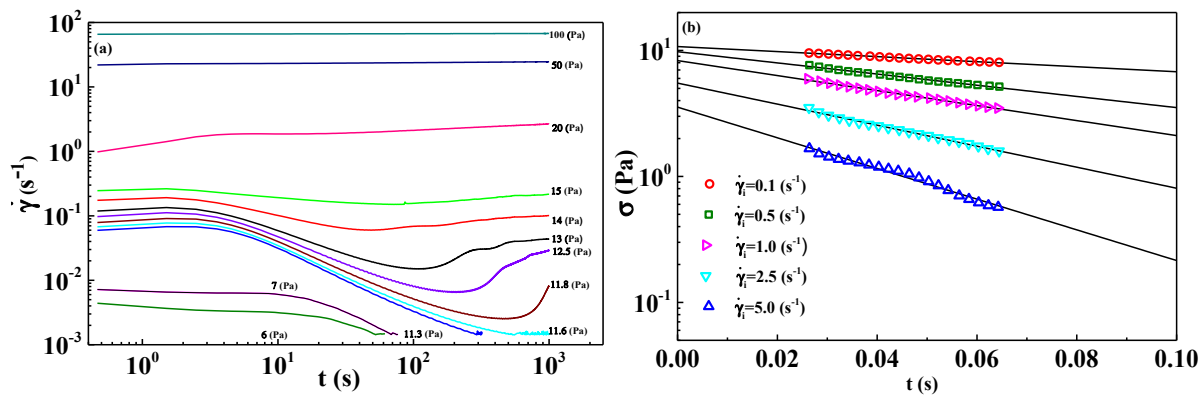


Figure S.1: (a) Static yield stress experiments with TA Instrument Discovery Hybrid Rheometer (40mm cone; 0.04 cone angle); (b) Stress jump experiments with 5 different initial shear rates to calculate σ_e following the procedure of Dullaert and Mewis (2005d) [Dullaert and Mewis (2005d)].

2) MDTM Fitting

Amplitude sweeps at two different frequencies ($\omega = 1, 10 \text{ rad/s}$) are shown with MDT model predictions, where the red line that denotes the critical strain, γ_{CO} in Fig. S.2. Below this, Fig. S.3 shows the 15 separate MDT model fits to the steady state shear data, and two sets of transient experiment data.

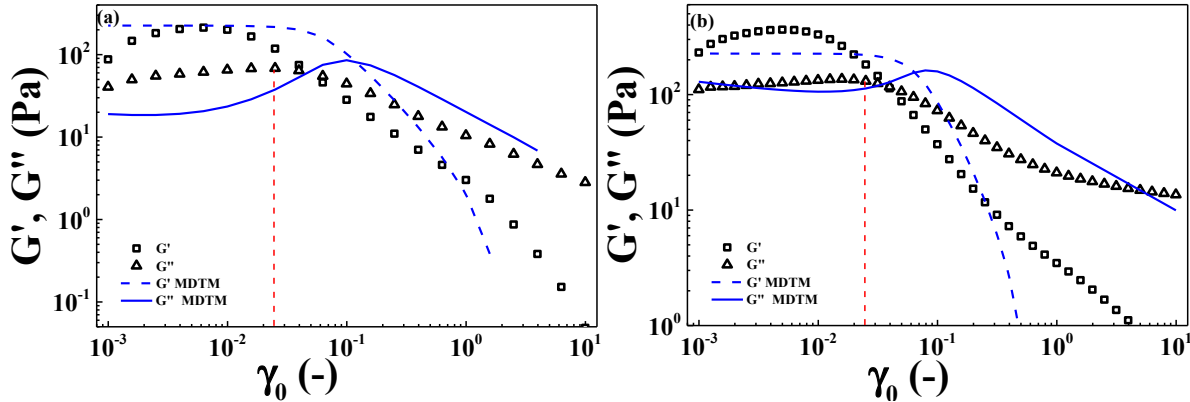


Figure S.2: Dynamic moduli as functions of strain amplitude for two different frequencies: (a) $\omega = 1 \text{ rad/s}$; (b) $\omega = 10 \text{ rad/s}$. Critical strain, γ_{CO} (2.4%) is indicated by the red dashed line calculated via σ_{y0} / G_0 using the best determined parameter values for the MDT model.

Fifteen independent trials of the parallel tempering algorithm [Armstrong *et al.* (submitted)] were performed from random initial guesses to find the optimum parameter values over the sets of steady state and transient data. Table S.1 shows the best parameter values from each run, and these model fits are plotted for the steady state, a step down, and a step up in shear rate test in Figure S.3. To further analyze the model behavior, the correlation matrix for these parameters is calculated using the Matlab inbuilt *corrcoef* command [Matlab (2013)], which also calculates the p-value. For the purpose of this discussion we follow the interpretation of correlation coefficient rules shown in Table S.2 such that values less than 0.35 in magnitude indicate no correlation, and the sign indicating positive or negative correlation. Starting at the top in Table S.3, K_{ST} , the structural consistency parameter is found to be moderately correlated with t_{r1} , and inversely correlated with n_2 , a and k_G . The p-value in parenthesis inform the significance of the correlation, where p-values less than 0.05 are deemed significant. Another strong positive correlation is between \hat{t}_{r1} and \hat{t}_{r2} . This implies that these thixotropic time constants are not truly independent of each other. Similarly, k_{Brown} is strongly correlated with \hat{t}_{r2} , and moderately correlated with \hat{t}_{r1} , again implying that fewer parameters may be able to effectively fit this set of experimental data. Lastly we mention that n_2 and k_G are moderately correlated, and this behavior may be due to the fact that this model is based on a Herschel-Bulkley form.

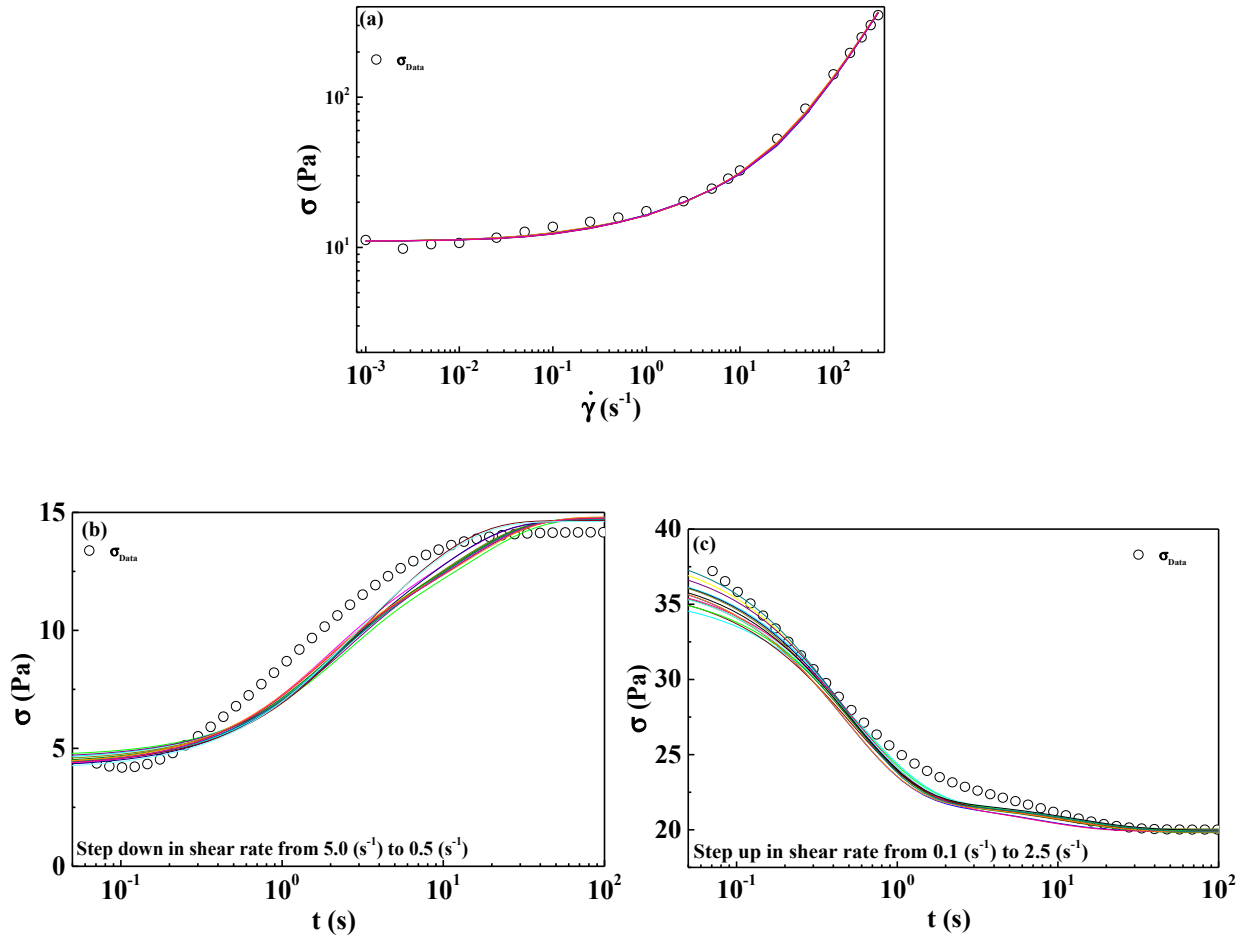


Figure S.3: Comparison of MDT model fits showing all 15 iterations of best parameter values to experimental steady state and transient shear data: (a) Steady state flow curve; (b) Step down in shear rate from 5 s^{-1} to 0.5 s^{-1} ; (c) Step up in shear rate from 0.1 s^{-1} to 2.5 s^{-1} .

Table S.1: Results of parallel simulated annealing of 15 iterations using MDT model. Run 8 is the optimal parameter set used in the manuscript.

Iteration	K_{Brown}	\hat{t}_{r1}	\hat{t}_{r2}	K_{ST}	a	k_G	n_2	d	Error
1	0.31	0.76	2.28	10.93	1.58	0.14	0.86	0.62	0.0656
2	0.23	0.77	2.70	10.82	1.52	0.07	0.80	0.63	0.0651
3	0.26	0.92	3.15	12.19	1.52	0.07	0.81	0.61	0.0650
4	0.21	0.99	4.55	11.97	1.49	0.08	0.79	0.59	0.0650
5	0.29	0.79	2.25	11.49	1.52	0.08	0.82	0.61	0.0648
6	0.27	0.87	5.24	11.43	1.44	0.10	0.83	0.54	0.0658
7	0.30	0.82	2.31	12.01	1.46	0.08	0.81	0.57	0.0648
8	0.28	0.77	2.08	11.21	1.53	0.09	0.81	0.65	0.0647
9	0.28	0.76	3.30	10.52	1.55	0.11	0.85	0.55	0.0658
10	0.21	0.85	3.87	11.03	1.52	0.08	0.80	0.59	0.0651
11	0.28	0.73	2.08	10.92	1.52	0.15	0.83	0.60	0.0655
12	0.29	0.81	2.40	11.40	1.55	0.08	0.81	0.65	0.0648
13	0.28	0.77	3.04	10.91	1.50	0.08	0.83	0.54	0.0654
14	0.34	0.79	1.50	12.47	1.47	0.07	0.80	0.65	0.0647
15	0.36	0.68	1.61	11.20	1.47	0.08	0.83	0.54	0.0654

Table S.2: Correlation Coeffient Interpretation [Taylor (1990)].

Correlation coefficient magnitude	Meaning
<0.35	weak
0.35 - 0.67	modest
0.68 - 0.89	strong
>0.9	very strong

Table S.3: Correlation Matrix for MDT model Parameters (p-values in parentheses; green color represents correlation; orange denotes self-correlation).

	K_{ST}	t_{r1}	t_{r2}	k_{Brown}	k_G	n_2	a	d
K_{ST}	1.00							
t_{r1}	0.56 (0.03)	1.00						
t_{r2}	-0.05	0.79 (0.00)	1.00					
k_{Brown}	0.13	-0.65 (0.01)	-0.88 (0)	1.00				
k_G	-0.49	-0.33	-0.09	0.16	1.00			
n_2	-0.54 (0.04)	-0.55 (0.03)	-0.29	0.49	0.74 (0)	1.00		
a	-0.55 (0.03)	-0.27	0.03	-0.17	0.43	0.33	1.00	
d	0.19	-0.08	-0.29	0.00	-0.12	-0.38	0.54	1.00

3) SSTM, Simple Scalar Thixotropy Model, Description and Fitting

For comparison we present the fitting results using the Simple Scalar Thixotropic Model (SST model) from [Colloidal Suspension Rheology](#) by Mewis and Wagner (2012). The SST model can be considered a “bare bones” version of the MDT model, with only 5 parameters. The stress expression,

$$\sigma = \lambda \sigma_{y0} + \lambda \eta_{ST} \gamma + \eta_\infty \gamma, \quad (\text{S.1})$$

and the structural evolution equation,

$$\frac{d\lambda}{dt} = k_{Brown} \left[-t_{r1} \lambda |\gamma| + (I - \lambda) \right], \quad (\text{S.2})$$

represent the SST model set and they are reduced versions of the respective stress and structural evolution equations of the MDT model. The structure kinetics equation includes two terms: one

term for shear breakage, and the other for Brownian build-up. The characteristic thixotropic time scale is:

$$t_{rl} = \frac{k_{Break}}{k_{Brown}}. \quad (\text{S.3})$$

Of the 5 parameters, σ_{y0} and η_∞ are directly fit to the steady state flow curve a priori. The other three are determined using the parallel simulated annealing algorithm applied to the 16 sets of step-up and step-down and the steady state flow curve. Comparison fits to the steady state flow curve, SAOS and the single step-up and step-down experiments are shown in Fig. S.4 and Fig. S.5 respectively. The best fit parameter values, and parameter correlation matrix are shown in Table S.4, and Table S.5 respectively. This is the simplest model, which incorporates only one thixotropic time scale.

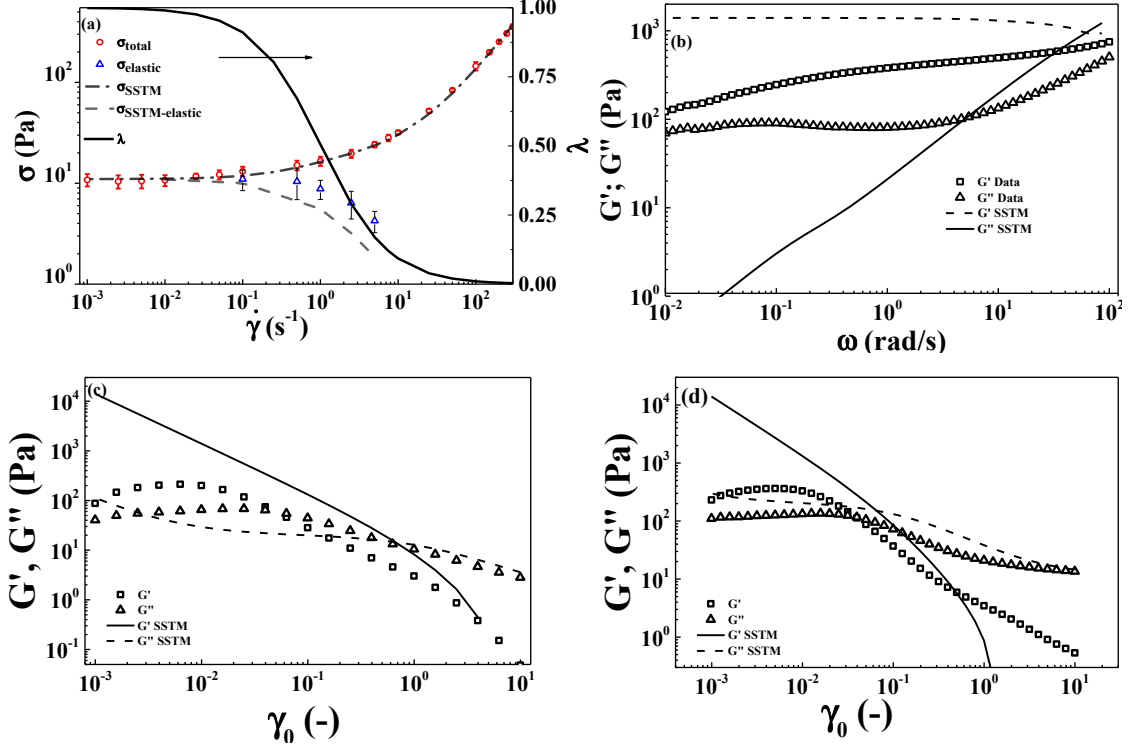


Figure S.4: Comparison of SST model fits to experimental data: (a) Steady state flow curve; (b) Small amplitude oscillatory shear (SAOS) frequency sweep at $\gamma_0 = 0.01$; (c) SAOS amplitude sweep at $\omega = 1$ rad/s; (d) SAOS amplitude sweep at $\omega = 10$ rad/s. (Parameter values listed in Table S.4).

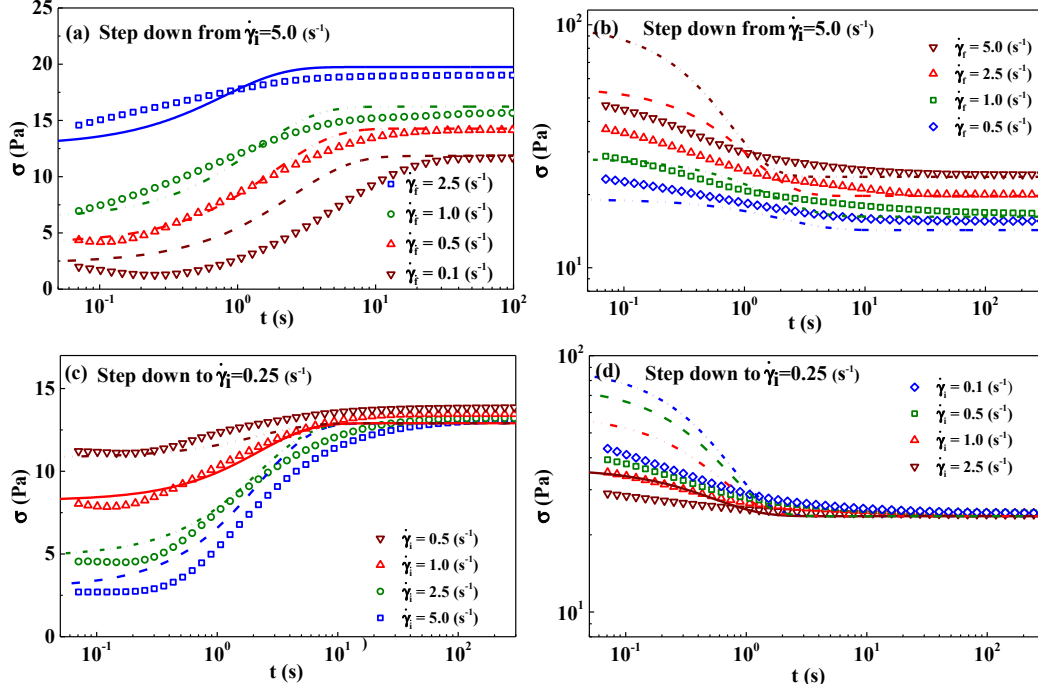


Figure S.5: Comparison of SST model fits with the parameter values in Table S.4 to experimental transient shear data: (a) Step down in shear rate from 5.0 s^{-1} ; (b) Step up in shear rate from 0.1 s^{-1} ; (c) Step down to 0.25 s^{-1} ; (d) Step up to 5.0 s^{-1} .

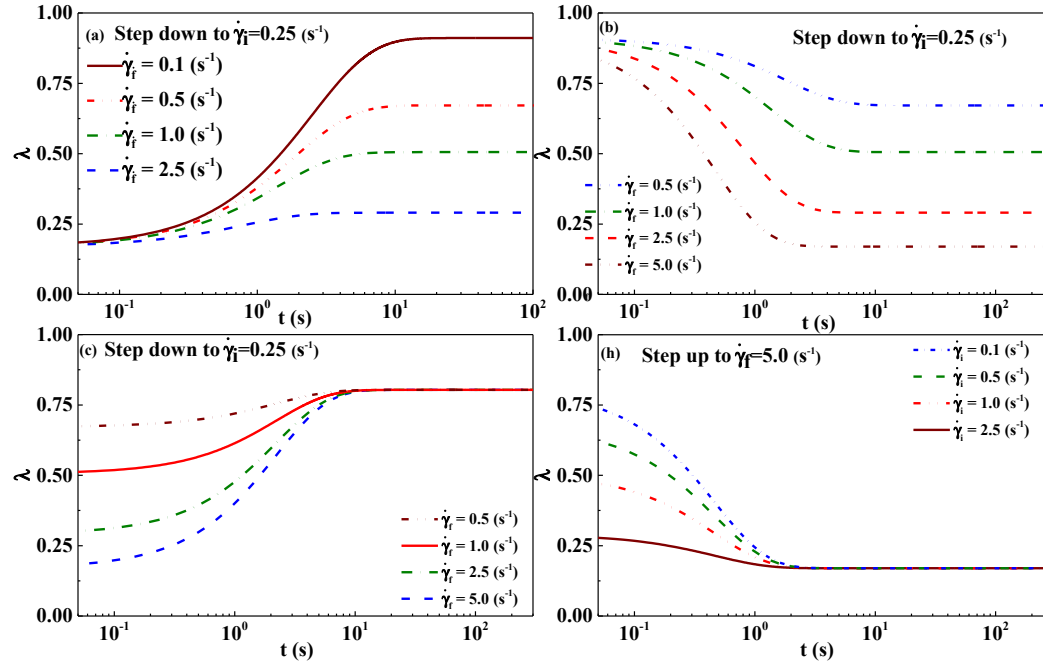


Figure S.6: SST model structure predictions with the parameter values in Table S.4 for: (a) Step down in shear rate from 5.0 s^{-1} ; (b) Step up in shear rate from 0.1 s^{-1} ; (c) Step down to 0.25 s^{-1} ; (d) Step up to 5.0 s^{-1} .

Table S.4: Parameter Values Determined for SST model.

Parameter	Units	Meaning	Range Initial Guess	Limiting Values	Optimum	Average	Range (+/-)
η_∞	Pa s	Infinite shear viscosity	(-)	(-)	1.17	(-)	(-)
$\sigma_{y\theta}$	Pa	Yield stress	(-)	(-)	11	(-)	(-)
η_{ST}	Pa s	Structural viscosity	[14 - 17]	>0	18.78	17.03	2
t_{rl} (k_{break}/k_{Brown})	s	Characteristic breakdown time	[1e ⁻³ - 1]	>0	0.98	0.87	0.08
k_{Brown}	s ⁻¹	Brownian time scale	[1e ⁻³ - 1]	>0	0.36	0.42	0.04

The correlation matrix for the SST model parameters (Table S.5) shows that there are two moderate correlations, and one strong correlation. It is easier to interpret these results due to the fact that only three parameters are investigated. The structural viscosity, η_{ST} is very strongly correlated with the first thixotropic time constant t_{rl} . This is due to the fact that together they act to control the contribution of the structural viscosity term, and are not independent of each other. In fact k_{Brown} is moderately correlated with both of them. As the value of k_{Brown} is adjusted in one direction, the structural viscosity and t_{rl} , which is inversely proportional to k_{Brown} , compensate to best fit the data.

Table S.5: Correlation Matrix for SST model Parameters (p-values in parenthesis, green color represents correlation; orange marks where parameter intersects itself in Correlation Matrix).

	η_{ST}	t_{rl}	k_{Brown}
η_{ST}	1.00		
t_{rl}	0.97 (0.02)	1.00	
k_{Brown}	-0.66 (0.04)	-0.67 (0)	1.00

4) Unified Approach Model Description and Fitting

The UA model employs a modified Jeffreys model as detailed in the text Dynamics of Polymeric Liquids, by Bird *et al.* (1987). The original equation was developed for polymeric solutions, and was imbued with two rheological time constants, a relaxation time (characteristic time of recovery) and a retardation time (characteristic time of loading). The original model requires specification of a polymer viscosity and a solvent viscosity, as well as a characteristic elastic modulus. The original Jeffreys model is shown in Eq. (S.4) in its scalar form where λ_1 , and λ_2 are the relaxation and retardation time respectively and η_0 is the zero shear viscosity,

$$\sigma + \lambda_1 \dot{\sigma} = \eta_0 (\gamma + \lambda_2 \dot{\gamma}). \quad (\text{S.4})$$

De Souza and Thompson modify the original Jeffreys model by adding characteristic times that are a function of current viscosities, which are in turn a superposition of the viscous contribution from the structure, and a viscous contribution from the pure solvent. In addition, an equilibrium viscosity η_{eq} ,

$$\eta_{eq} = \left[I - \exp\left(-\frac{\eta_0 \gamma_{eq}}{\sigma_y}\right) \right] \left\{ \frac{\sigma_y - \sigma_{yd}}{\gamma_{eq}} e^{-\gamma_{eq}/\gamma_{yd}} + \frac{\sigma_{yd}}{\gamma_{eq}} + K \gamma_{eq}^{n-1} \right\} + \eta_\infty, \quad (\text{S.5})$$

is included, which is updated as necessary to reflect current flow conditions. The equilibrium viscosity consists of η_0 , η_∞ , zero-shear, and infinite shear viscosity, σ_y , σ_{yd} , the static and dynamic yield stress, K , consistency parameter, n power law exponent, and γ_{yd} , representing the transition shear rate of the yield stress. The structure evolution equation depends in part on the difference between the current viscosity and equilibrium viscosity. This difference is a driving force that drives structural evolution, and is calculated implicitly from the instantaneous stress.

$$\gamma + \theta_2 \dot{\gamma} = \frac{\theta_2}{\eta_\infty} \left(\frac{\sigma}{\theta_1} + \sigma \right) \quad (\text{S.6})$$

is the modified constitutive equation with θ_1 and θ_2 which represent the relaxation, and retardation times respectively:

$$\theta_1 = \left(I - \frac{\eta_\infty}{\eta_v(\lambda)} \right) \frac{\eta_v(\lambda)}{G_v(\lambda)}, \quad (\text{S.7})$$

$$\theta_2 = \left(I - \frac{\eta_\infty}{\eta_v(\lambda)} \right) \frac{\eta_\infty}{G_v(\lambda)}. \quad (\text{S.8})$$

This model requires the solution of two ordinary differential equations, one for structure:

$$\frac{d\lambda}{dt} = \frac{1}{t_{eq}} \left[\left(\frac{1}{\lambda} - \frac{1}{\lambda_0} \right)^a - \left(\frac{\lambda}{\lambda_{eq}} \right)^b \left(\frac{1}{\lambda_{eq}} - \frac{1}{\lambda_0} \right)^a \right], \quad (\text{S.9})$$

and another for either shear rate or stress (depending if the experiment to be fit was strain or stress controlled). A more detail description of this model can be found in literature [de Souza Mendes and Thompson (2013); de Souza Mendes (2009)]. The model is presented in versions with either seven or nine parameters, with the difference being specification of both a static and dynamic yield stress with a parameter that dictates the transition shear rate between the two values replacing a simple yield stress. The ancillary algebraic equations are shown in Eq. (S.10) through Eq. (S.14),

$$G_v(\lambda) = G_0 e^{m \left(\frac{1}{\lambda} - \frac{1}{\lambda_0} \right)}, \quad (\text{S.10})$$

$$\eta_v(\lambda) = \eta_\infty e^\lambda, \quad (\text{S.11})$$

$$\lambda_{eq} = \ln \left(\frac{\eta_{eq}}{\eta_\infty} \right), \quad (\text{S.12})$$

$$\lambda_0 = \ln \left(\frac{\eta_0}{\eta_\infty} \right), \quad (\text{S.13})$$

$$\sigma_{eq} = \eta_{eq}(\sigma) \gamma_{eq}. \quad (\text{S.14})$$

Importantly, as this model is implicit in the stress, the solution of Eq. (S.14) is required for every time step, and during every Runge-Kutta step for the differential equation solution. Note that Eq. (S.14) represents an equilibrium, or steady state value if the stress was allowed to attain steady state at its current value. The UA model has both thixotropic and viscoelastic characteristics.

Comparison fits to the steady state flow curve, SAOS and the single step-up and step-down experiments are shown in Fig. S.7 and Fig. S.8 respectively. The best fit parameter values and parameter correlation matrix shown in Table S.6, and Table S.7 respectively.

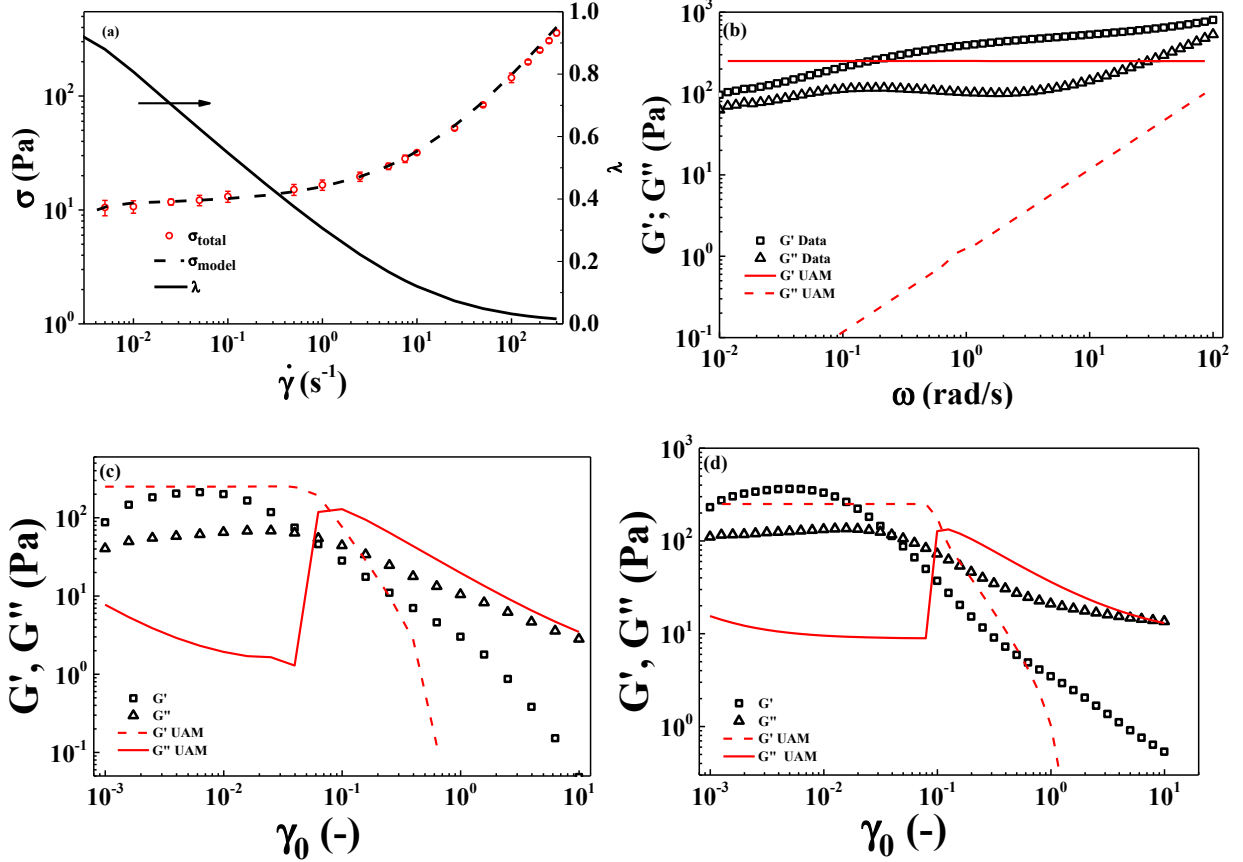


Figure S.7: Comparison of UA model fits to experimental data: (a) Steady state flow curve; (b) SAOS frequency sweep at $\gamma_0 = 0.01$; (c) SAOS amplitude sweep at $\omega = 1$ rad/s; (d) SAOS amplitude sweep at $\omega = 10$ rad/s data and predictions using UAM. (Parameters from Table S.6).

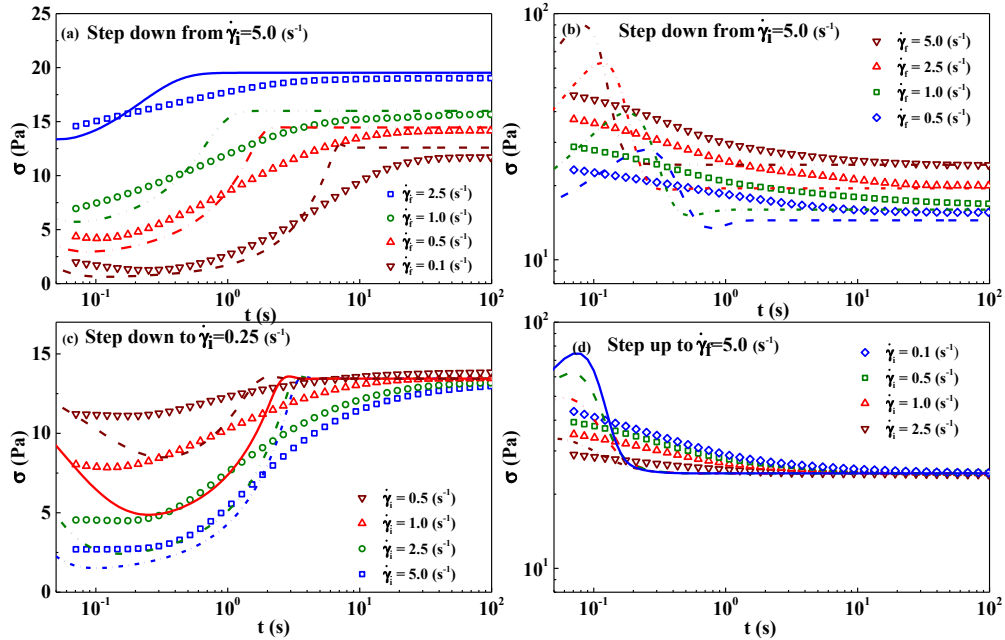


Figure S.8: Comparison of UA model fits with parameter values from Table S.6 to experimental transient shear data: (a) Step down in shear rate from 5.0 s^{-1} ; (b) Step up in shear rate from 0.1 s^{-1} ; (c) Step down to 0.25 s^{-1} ; (d) Step up to 5.0 s^{-1} .

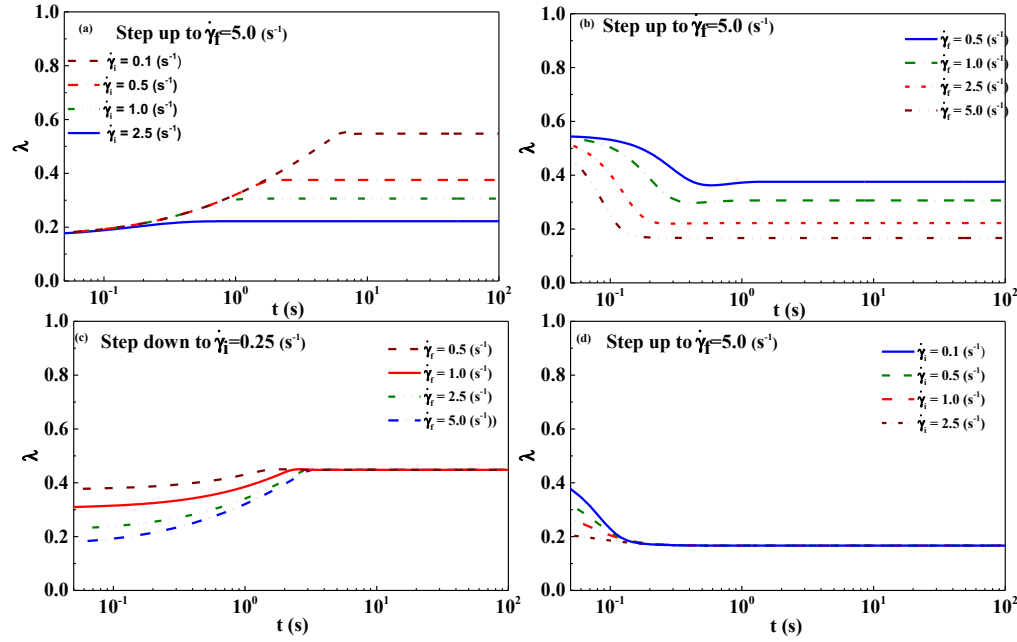


FIG S9: UA model structure predictions with the parameter values in Table S.6 for: (a) Step down in shear rate from 5.0 s^{-1} ; (b) Step up in shear rate from 0.1 s^{-1} ; (c) Step down to 0.25 s^{-1} ; (d) Step up to 5.0 s^{-1} .

Table S.6: Parameter Values Determined for UA model.

Parameter	Units	Meaning	Range Initial Guess	Limiting Values	Optimal	Average	Range (+/-)
η_0	$\text{Pa}\cdot\text{s}$	zero Shear viscosity	(-)	>0	6000	(-)	(-)
σ_{y0}	Pa	yield stress	(-)	>0	8	(-)	(-)
η_∞	$\text{Pa}\cdot\text{s}$	infinite shear viscosity	(-)	>0	2.9	(-)	(-)
G_0	(Pa)	elastic modulus	(-)	>0	800	(-)	(-)
K	$\text{Pa}\cdot\text{s}^n$	consistency parameter	[2, 5]	>0	4.07	4.17	0.16
n	(-)	power law exponent	[1e-3, 1]	>0	0.82	0.82	0.06
m	(-)	elastic modulus constant	[1e-3, 1]	>0	0.11	0.20	0.06
a	(-)	structure build up power law exponent	[1e-3, 2]	>0	0.91	0.92	0.12
b	(-)	structure break down power law exponent	[1e-3, 2]	>0	1.11	1.13	0.14
t_{eq}	s	characteristic time of structure change	[1e-3, 1]	>0	3.420	3.010	0.5

With respect to the correlation matrix of the UAM it is noteworthy that the consistency parameter and power law exponent are strongly, positively correlated. This is to be expected due to the fact that those physical terms nature of the equilibrium viscosity equation. In addition n is negatively correlated with b , and positively correlated with m . Lastly, K is positively correlated with b and negatively correlated with m . This may also imply that there may exist a better way to construct the structural evolution equation. Although when comparing the correlations to the SST model and MDT model in general there are many fewer correlations between parameters.

Table S.7: Correlation Matrix for UA Model Parameters (p-values shown in parenthesis green color represents correlation; orange marks where parameter intersects itself in Correlation Matrix).

	t_{EQ}	n	K	a	b	m
t_{EQ}	1.00					
n	-0.13	1.00				
K	-0.09	-0.96 (0)	1.00			
a	-0.42	0.13	0.07	1.00		
b	0.13	-0.51 (0.05)	0.52 (0.05)	0.40	1.00	
m	0.05	0.56 (0.03)	-0.54 (0.04)	0.14	-0.06	1.00

6) Bautista – Manero –Puig Model Description and Fitting

The model is based on fluidity additivity, and is employed here using five relaxation modes based on the minimum number of modes required to accurately represent the SAOS frequency sweep data shown in Figure S.11. The equations are presented in tensorial form. In these equations the i subscripts represent the number of the relaxation mode. For each mode, the corresponding fluidity (=inverse of viscosity) obeys a relaxation equation

$$\frac{d\varphi_i}{dt} = \frac{(\varphi_{0,i} - \varphi_i)}{\lambda_i} + k_i(\varphi_{\infty,i} - \varphi_i)\boldsymbol{\sigma} : \mathbf{D}, \quad (\text{S. 15})$$

where $\boldsymbol{\sigma}$ is the total stress $\boldsymbol{\sigma} = \sum_{i=1}^N \boldsymbol{\sigma}_i$ and the $\boldsymbol{\sigma}_i$ is the i th mode stress contribution, each one of which obeys a generalized Maxwell equation

$$\boldsymbol{\sigma}_i + \delta_i \nabla \cdot \boldsymbol{\sigma}_i = \frac{2\mathbf{D}}{\varphi_i}. \quad (\text{S. 16})$$

Eq. (S.15) and Eq. (S.16) show the general tensorial form. The model relaxation moduli and respective relaxation times (for all five relaxation modes) are directly fit to small amplitude oscillatory shear data, while the fluidity evolution parameters are fit to 16 sets of transient and one set of steady state data simultaneously. Comparison fits to the steady state flow curve, SAOS and a the step-up and step-down experiments are shown in the Fig. S.11 and Fig. S.12 respectviely. The best fit parameter values and parameter correlation matrix shown in Table S.8, and Table S.9 respectively. Our use of this model explores the ability to fit and predict thixotropic suspension viscosity using an equation without a traditional “structure parameter” term, but rather with a

Delete
Delete
Forma
spellin
Forma
spellin

fluidity that is allowed to evolve via an evolutionary equation [Bautista *et al.* (1999)]. One will note that limitations of this ad-hoc procedure to model the fluidity yield SAOS predictions that are shown in Fig. S.11b-d that are not entirely consistent with the experimental data.

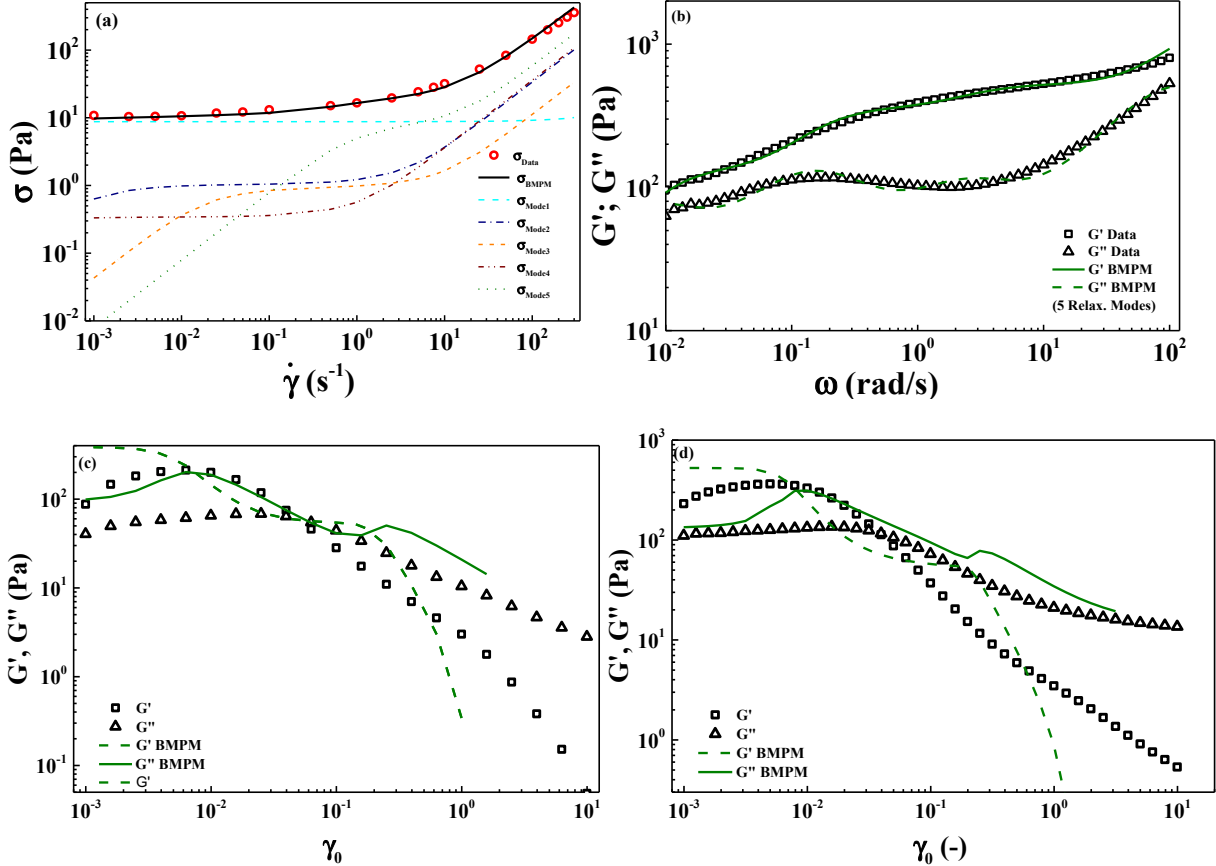


Figure S.11: Comparison of 5-mode BMPM fits to experimental data: (a) Steady state flow curve; (b) SAOS frequency sweep at $\gamma_0 = 0.01$; (c) SAOS amplitude sweep at $\omega = 1$ rad/s; (d) SAOS amplitude sweep at $\omega = 10$ rad/s. The 5-Mode BMP model parameter values are listed in Tables S.8 & S.9.

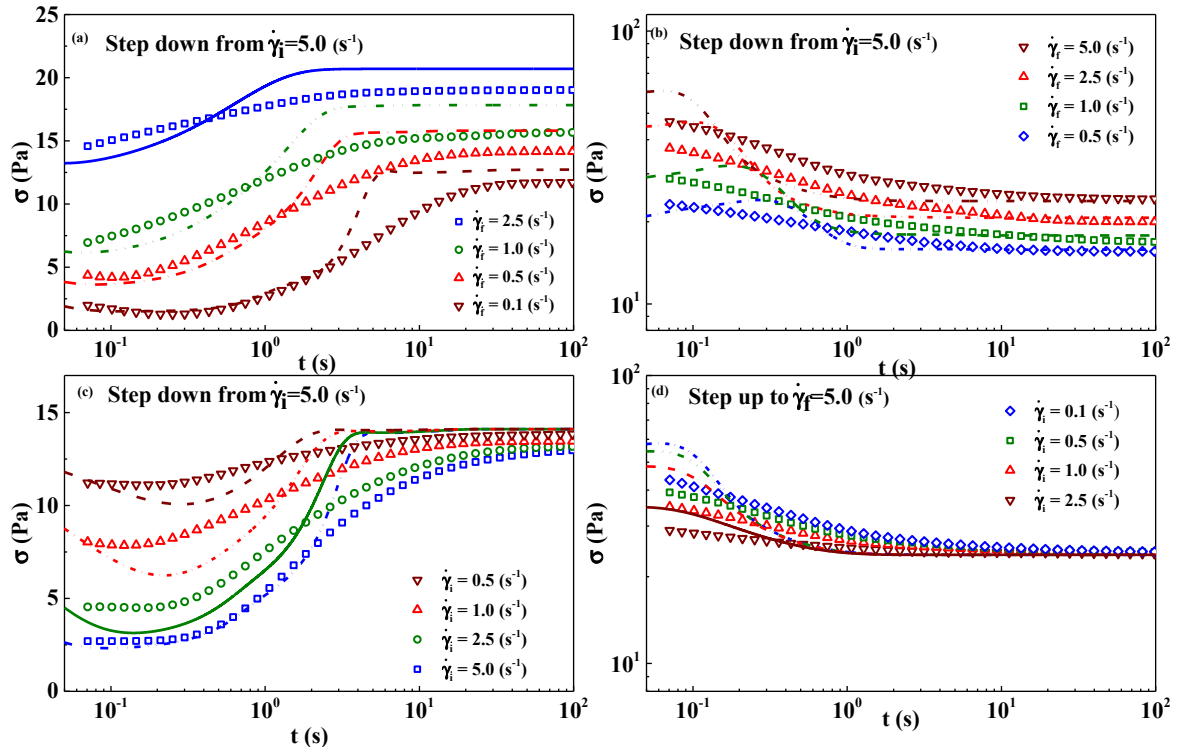


Figure S.12: Comparison of 5-mode BMPM fits to experimental transient shear data: (a) Step down from 5 s^{-1} to 4 different values as indicated ; (b) Step up from 0.1 s^{-1} ; (c) Step down to 0.25 s^{-1} ; (d) Step up to 5.0 s^{-1} . The 5-Mode BMP model parameter values are listed in Tables S.8 & S.9.

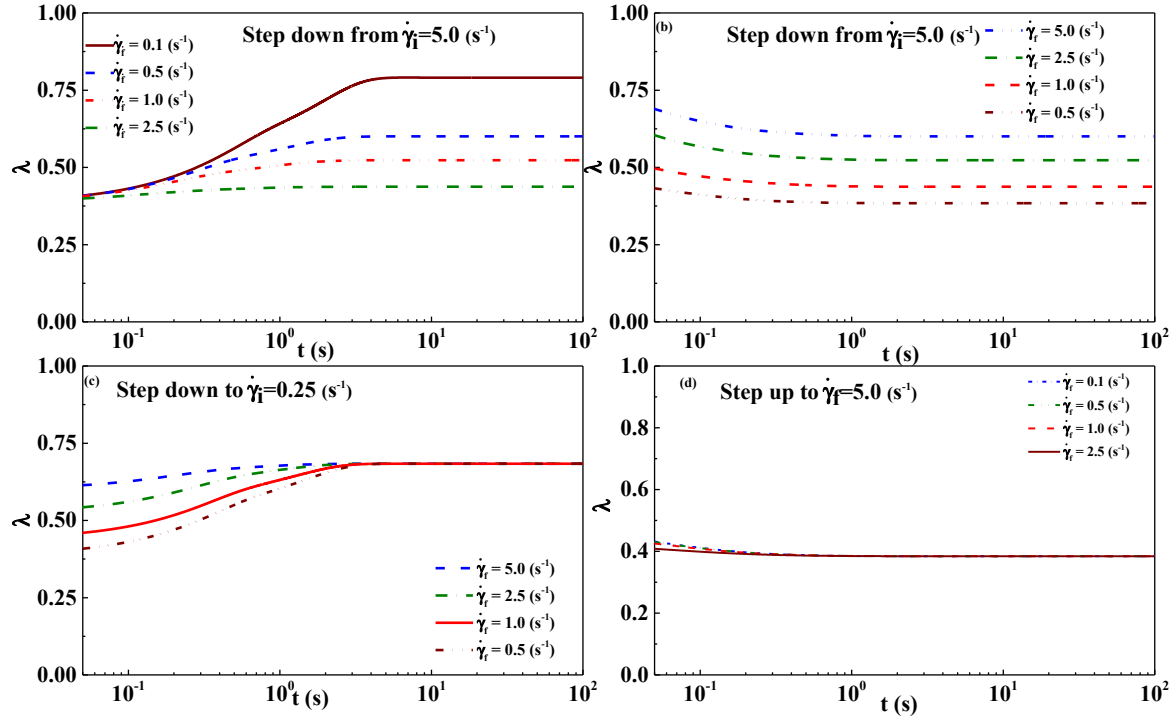


Figure S.13: 5-mode BMP model structure predictions for: (a) Step down in shear rate from 5.0 s^{-1} to 4 different values as indicated; (b) Step up in shear rate from 0.1 s^{-1} ; (c) Step down to 0.25 s^{-1} ; (d) Step up to 5.0 s^{-1} . The 5-Mode BMP model parameter values are listed in Tables S.8 & S.9.

Table S.8: BMP model “best fit” relaxation spectrum values of 5-mode stress relaxation.

Parameter	Units	Meaning	Limiting Values	Optimal
G_i	Pa	Elastic modulus of mode i	>0	57.0
				213.4
				151.2
				116.3
				1053.5
τ_i	s	Relax. time of fluidity of mode i	>0	1.00E+100
				4.7
				0.28
				53.7
				7.50E-03
φ_{oi}	$(\text{Pa s})^{-1}$	Infinite shear fluidity mode i	>0	1.75E-02
				9.90E-04
				2.30E-02
				1.60E-04
				1.30E-01

Table S.9: BMP model “best fit” parameter values.

Parameter	Units	Meaning	Range Initial Guess	Limiting Values	Optimal	Average	Range (+/-)
k_1	Pa^{-1}	multiplier for the fluidity "increase" term (aka the structural breakage term)	[1E-7 1E-5]	>0	5.97E-05	8.54E-05	3.91E-05
k_2			[1E-3 1E-1]		0.43	0.28	0.061
k_3			[1E-2 1]		0.71	0.61	0.15
k_4			[1 10]		8.28	9.26	4.68
k_5			[1E-3 1E-1]		0.10	0.13	0.073
λ_1	s	relaxation time of change in fluidity	[1E-1 1E+1]	>0	1.28	1.23	0.12
λ_2			[1E-1 10]		0.47	1.11	0.91
λ_3			[1E-1 10]		0.249	0.209	6.68E-02
λ_4			[1E-1 10]		0.47	0.33	0.15
λ_5			[1E-1 10]		6.52E-02	7.46E-02	0.017
φ^∞_1	$(\text{Pa s})^{-1}$	infinite shear fluidity	[1E+3 1.5E+3]	>0	147.72	1.24E+02	6.76E+01
φ^∞_2			[1 10]		5.27	2.97	0.67
φ^∞_3			[1 10]		2.7	8.96	5.54
φ^∞_4			[1 10]		2.38	2.78	0.59
φ^∞_5			[1 10]		2.59	1.72	0.36

7) LAOS, Flow Reversal and UD-LAOS Prediction Comparison with all Models

Below we use the best global fit model parameters for the SST model, MDT model, UA model and BMP model to compare how each performs in *predicting* LAOS flow. Fig. S.14 shows an elastic and viscous projection comparison for $\omega=1 \text{ rad/s}$; $\gamma_0=1$, and $\omega=0.1 \text{ rad/s}$; $\gamma_0=1$ for each model, followed by a Pipkin space representation in Fig. S.15 comparing model predictions with the LAOS data for all conditions explored. Fig. S.16 shows flow reversal experiments for the solvent to gauge the performance of the instrument. Next, in Fig. S.17 we compare predictions for flow reversal for each model and observe a general failure to accurately predict the time-dependent shear stress, along with the respective structure predictions. The UD-LAOS stress is comparison to all model predictions is presented in Fig. S.18.

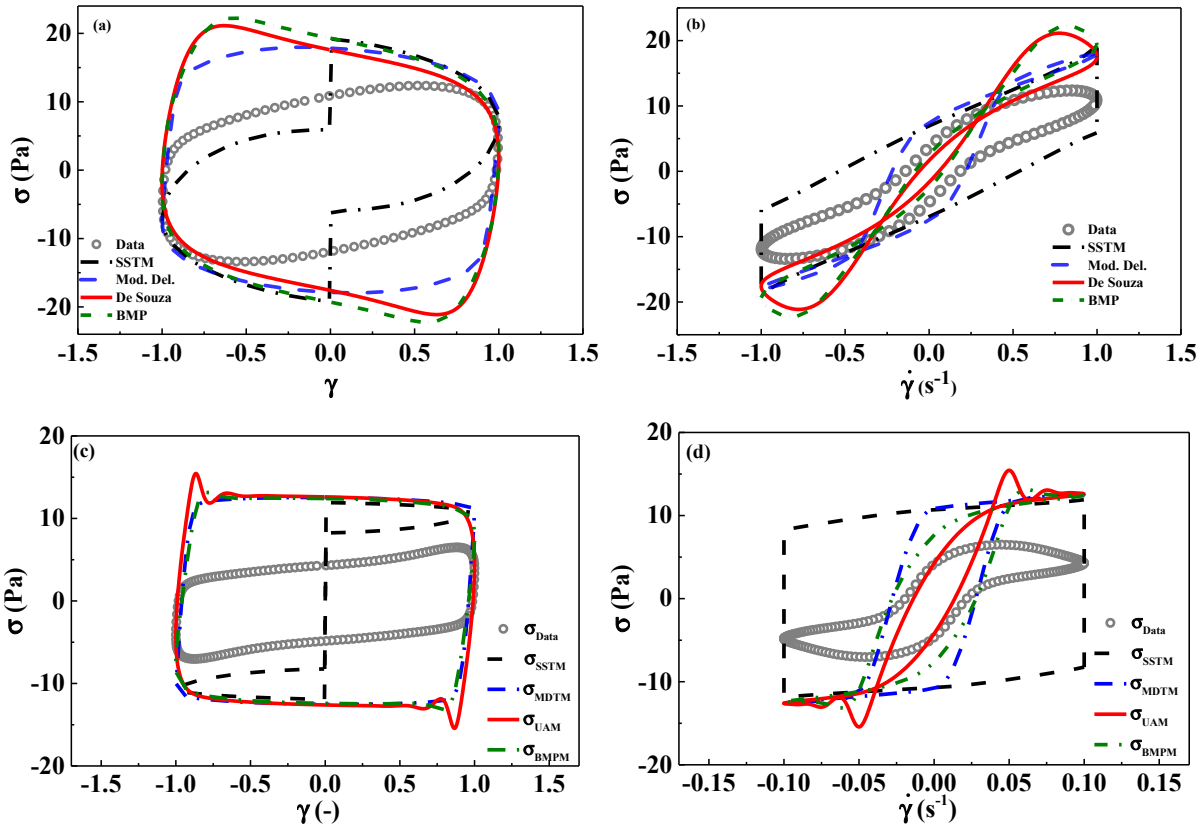


Figure S.14: (a) Elastic projection; (b) viscous projection $\omega = 1 \text{ rad/s}$; $\gamma_0 = 1$; (c) Elastic projection; and (d) Viscous projection of all four models at $\omega = 0.1 \text{ rad/s}$; $\gamma_0 = 1$. All model comparison using best fit parameters.

Table S.10: Maximum values of experimental stress during LAOS experiments (grid corresponds to 2-D Lissajous-Bowditch projections).

γ_0	$\sigma_{\text{exp}}(\text{Pa})$				
1000	27.1	141			
100	12.9	29.6	141		
10	10.8	15.0	29.4	140	
1	6.7	6.5	12.4	23.6	
0.1		3.9	7.5	8.6	
ω (rad/s)	0.01	0.1	1	10	

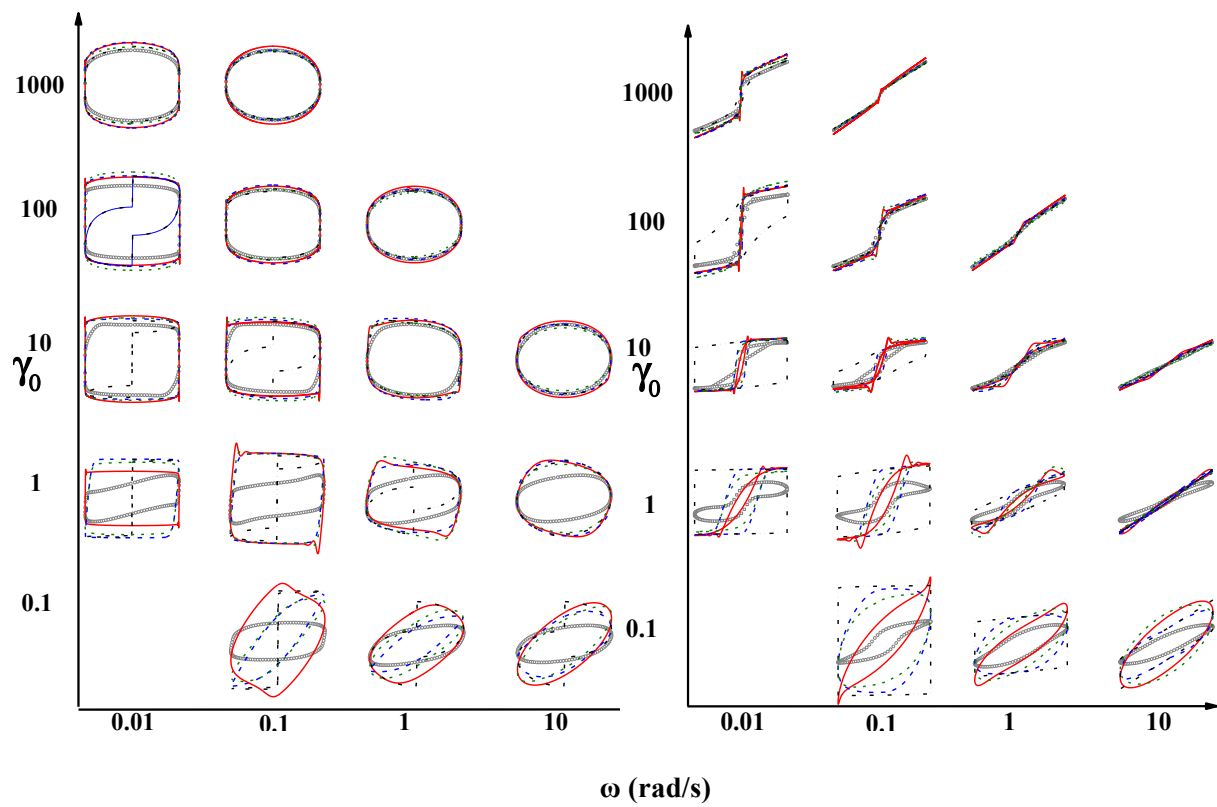


Figure S.15: (a) Elastic projections. (b) Viscous projections. All model comparison. Strain and shear rate made dimensionless with maximum values over cycle, stress made dimensionless with maximum experimental values of each cycle (Black SSTM; blue MDTM; red UAM; and green BMPM).

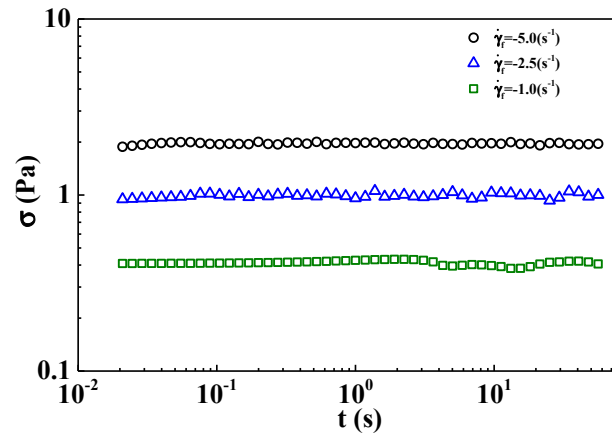


Figure S.16: Flow reversal experiments, stress vs. time of pure solvent (paraffin oil and PIB) for various shear rates.

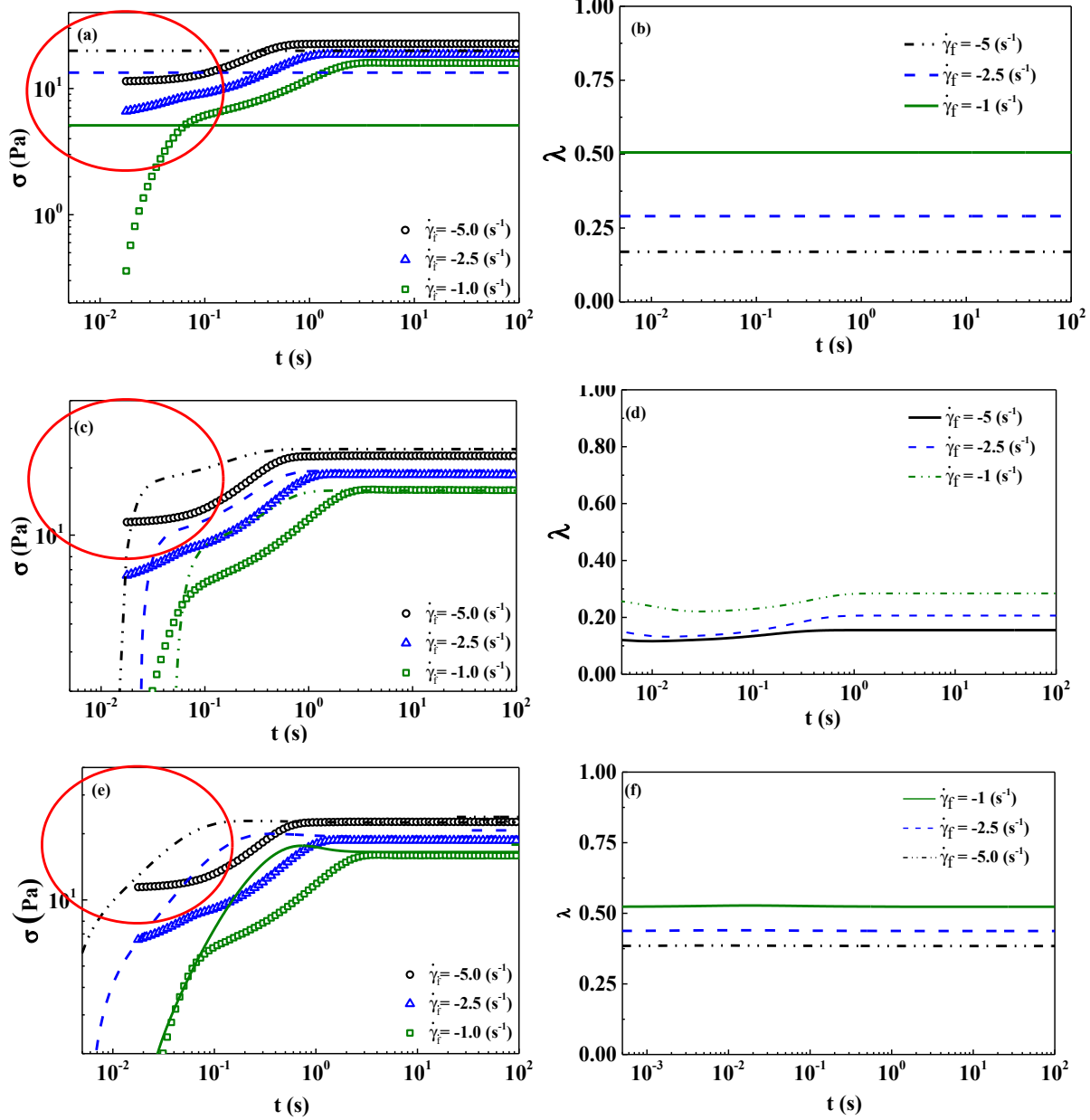


Figure S.17: (a) Flow reversal experiment and SST model predictions; (b) Corresponding λ values; (c) Flow reversal experiment and UA model predictions; (d) Corresponding λ values; (e) Flow reversal and BMP model predictions; (f) Corresponding λ values.

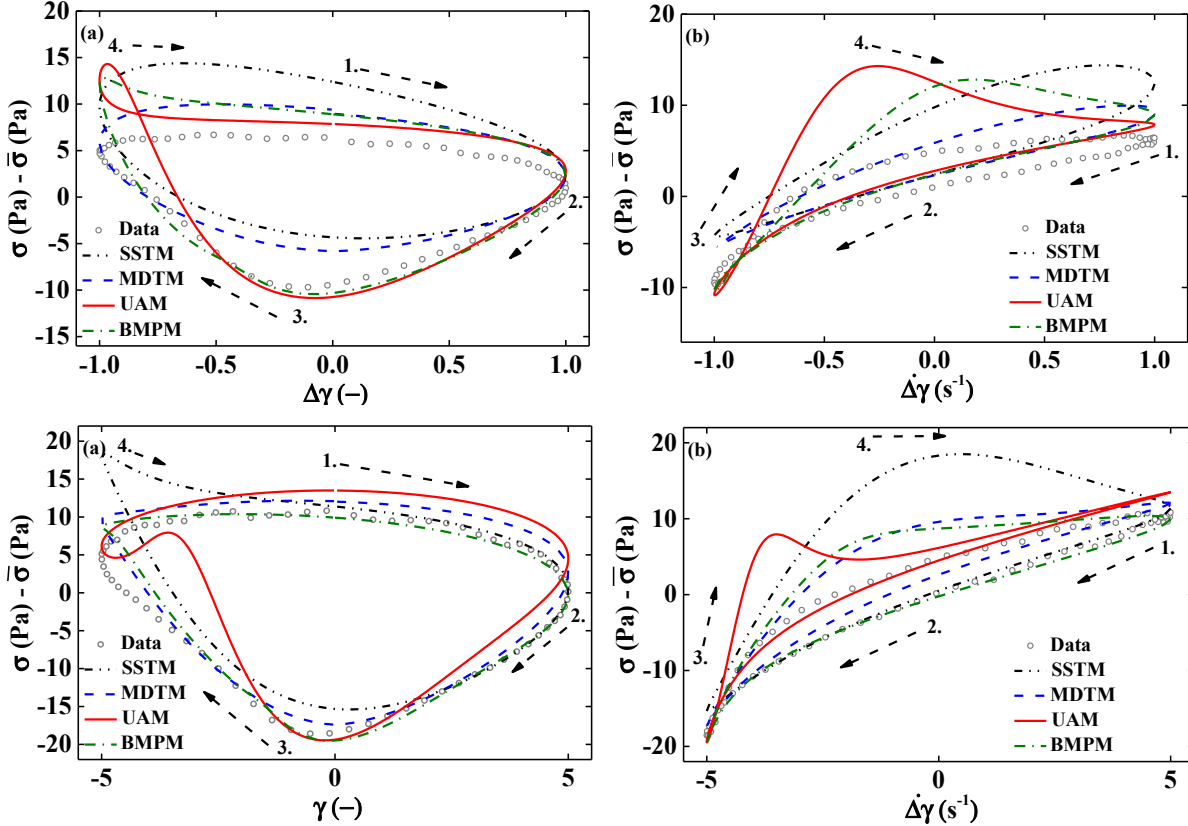


Fig S.18: UD-LAOS data compared to model predictions: (a) Elastic projections; (b) Viscous projections. Top row: $\omega = 1 \text{ rad/s}$; $\gamma_0 = 1$; with $\bar{\sigma} = 11.0 \text{ Pa}$. Bottom row: $\omega = 1 \text{ rad/s}$; $\gamma_0 = 5$; $\Delta\sigma = \sigma(t) - \bar{\sigma}(t)$ with $\bar{\sigma} = 19.6 \text{ Pa}$; $\Delta\gamma = \gamma(t) - \gamma_0\omega t$; $\dot{\gamma} = \dot{\gamma}(t) - \dot{\gamma}_0\omega$.

For reference, Figure S.19 shows the values of the average shear stress during UD-LAOS compared with the steady state flow curve. It can be observed that the average shear stress during UD-LAOS approximately follows that observed during steady shearing.

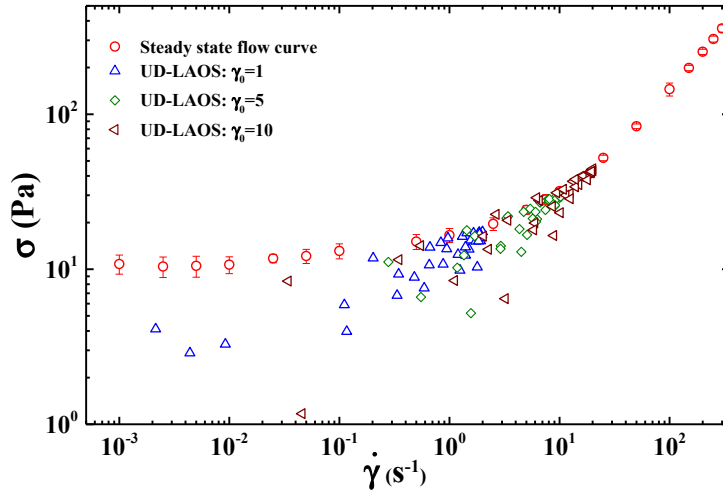


Fig S.19: Steady state flow curve data comparison to UD-LAOS data $\omega = 1 \text{ rad/s}$; $\gamma_0 = 1, 5, 10$.

References

- Armstrong, M. J., A. N. Beris, and N. J. Wagner, "Dynamic data-driven parameter estimation of nonlinear models based on a parallel simulated annealing method." *AIChE J.* (submitted).
- Bautista, F., J. M. de Santos, J. E. Puig, and O. Manero. "Understanding thixotropic and antithixotropic behavior of viscoelastic micellar solutions and liquid crystalline dispersions." *J. Non-Newtonian Fluid Mech.* **80**, 93 – 113 (1999).
- Bird, B. R., R. C. Armstrong, and O. Hassager. *Dynamics of Polymeric Liquids*. John Wiley and Sons, New York, NY (1987).
- de Souza Mendes, P.R. "Modeling the thixotropic behavior of structured fluids." *J. Non-Newtonian Fluid Mech.* **164**, 66-75 (2009).
- de Souza Mendes, P. R. and R. L. Thompson. "A unified approach to model elasto-viscoplastic thixotropic yield-stress materials and apparent yield-stress fluids." *Rheol. Acta* Vol. **52**, 673 – 694 (2013).
- Dullaert, K., and J. Mewis. "Stress jumps on weakly flocculated dispersions: Steady state and transient results". *J. Coll. Int. Sci.* **287**, 542-551 (2005d).
- Matlab, User Help Guide, The MathWorks Inc. (1994-2013).
- Mewis, J., and N. J. Wagner. *Colloidal Suspension Rheology*. Cambridge University Press, New York, Cambridge University Press (2012).
- Taylor, T., "Interpretation of the correlation coefficient: A basic 1212 review," *J. Diagn. Med. Sonography* 6, 35–39 (1990).